THE JOURNAL OF BIOLOGICAL CHEMISTRY
Vol. 277, No. 52, Issue of December 27, pp. 50914–50922, 2002

Printed in U.S.A.

Surface-catalyzed Amyloid Fibril Formation*

Received for publication, July 18, 2002, and in revised form, September 21, 2002
Published, JBC Papers in Press, September 27, 2002, DOI 10.1074/jbc.M207225200

Min Zhu‡, Pierre O. Souillac‡, Cristian Ionescu-Zanetti§, Sue A. Carter§, and Anthony L. Fink‡¶

From the ‡Department of Chemistry and Biochemistry and the §Department of Physics, University of California, Santa Cruz, California 95064

Light chain (or AL) amyloidosis is characterized by the pathological deposition of insoluble fibrils of immunoglobulin light chain fragments in various tissues, walls of blood vessels, and basement membranes. In the present investigation, the *in vitro* assembly of a recombinant amyloidogenic light chain variable domain, SMA, on various surfaces was monitored using atomic force microscopy. SMA formed fibrils on native mica at pH 5.0, conditions under which predominantly amorphous aggregates form in solution. Fibril formation was accelerated significantly on surfaces compared with solution; for example, fibrils grew on surfaces at significantly faster rates and at much lower concentrations than in solution. No fibrils were observed on hydrophobic or positively charged surfaces or at pH >7.0. Two novel types of fibril growth were observed on the surface: bidirectional linear assembly of oligomeric units, and linear growth from preformed amorphous cores. In addition to catalyzing the rate of fibrillation, the mechanism of fibril formation on the surfaces was significantly different from in solution, but it may be more physiologically relevant because *in vivo* the deposits are associated with surfaces.

Immunoglobin (Ig) light chains (LCs)[1] are involved in various protein deposition diseases, such as AL amyloidosis (also known as primary systemic amyloidosis or LC amyloidosis), LC deposition disease, myeloma cast nephropathy, and acquired Fanconi's syndrome (1–4). Ig LCs were found in vital organs in various morphologies, including fibrils, amorphous casts, basement membrane precipitates, and intracellular crystals (5, 6). The continuous accumulation of these insoluble forms leads to organ dysfunction and eventually to death. The molecular mechanisms leading to protein deposition are not well known. SMA belongs to the κIV family of Ig LCs, was extracted from lymph node-derived amyloid fibrils of an AL amyloidosis patient, and corresponds to the variable domain region. Our *in vitro* experiments with recombinant SMA (114 residues, 12.7 kDa) have demonstrated that the protein aggregates via partially folded intermediates to form ordered aggregates such as protofibrils and fibrils as well as disordered amorphous aggregates (7, 8). Earlier studies suggested that insoluble fibrils and amorphous protein deposits play a role in the molecular pathogenesis of amyloid disease (9–11); however, it has become increasingly evident that certain nonfibrillar forms, such as soluble or insoluble oligomers, possess toxic properties (12–15). Therefore, there is great interest in understanding the morphologies of LC domains on the aggregation pathway.

Previous work on the *in vitro* system focused predominantly on the morphological properties of SMA aggregates grown from solution. Because LCs are frequently found to deposit in arterial walls and basement membranes (2), interfacial phenomena and the interaction between protein and the surface may be involved in the aggregation process. In LC deposition disease the amorphous deposits are found associated with the basement membrane (16). The presence of 10-nm diameter LC amyloid fibrils along the epithelial basement membrane as well as in the vascular walls was ascertained by electron microscopy (2). There is at least one report of the association of SMA with cell membranes (17). The current work focuses on the morphologies of protein aggregates on surfaces.

At present, more than 18 different amyloidogenic proteins or peptides have been identified which are associated with protein deposition disease. These proteins share similar morphology of fibrils (18–21), all forming twisted, linear, Congo Red-binding fibrils, typically 5–10 nm in diameter with a crossed β-pleated sheet conformation. There is already some evidence that surfaces may be crucial for fibril formation of Aβ peptide. The size and the shape of Aβ peptide aggregates, as well as the kinetics of their formation, exhibited pronounced dependence on the physicochemical nature of the surface. On hydrophilic mica, Aβ peptide formed linear assemblies with an average height of 5–6 nm, whereas on hydrophobic graphite the Aβ peptide formed uniform, elongated sheets 1 nm in height (22). Fibrils of amylin formed on mica also exhibited different types of morphologies, lacking the twisted rope-like morphology seen in those grown in solution (23). Some proteins have been shown to interact with membranes, which may affect fibril formation (24–26). The involvement of surfaces could be universal for all amyloid-associated proteins. We have observed that the *in vitro* fibril formation of SMA is sensitive to the test tube materials and the nature of the beads used for stirring. This can be explained by surface interactions and subsequent conformation changes caused by the attachment of the protein to the surface. We have also observed that the fibrillation of α-synuclein, a protein associated with Parkinson's disease, depended on the nature of the surfaces present in the incubating solution. Therefore, the investigation of the surface dependence of fibril formation is also significant for the mechanism of fibril formation of other amyloid proteins.

AFM is a powerful technique for studying the morphology and structure of amyloid fibrils, with high resolution and imaging ability in air and fluid, *i.e.* dry or solution samples. Previously, we have monitored the fibril assembly of the Ig LC SMA in solution by AFM, and a model for fibril formation involving a hierarchical assembly process from protofilaments

* This work was supported by National Institutes of Health Grant DK55675 (to A. L. F.). The costs of publication of this article were defrayed in part by the payment of page charges. This article must therefore be hereby marked "*advertisement*" in accordance with 18 U.S.C. Section 1734 solely to indicate this fact.

¶ To whom correspondence should be addressed: Dept. of Chemistry and Biochemistry, University of California, 1156 High St., Santa Cruz, CA 95064. Tel.: 831-459-2744; Fax: 831-459-2935; E-mail: enzyme@cats.ucsc.edu.

[1] The abbreviations used are: LC(s), light chain(s); AFM, atomic force microscopy; ThT, thioflavin T.

(2.4 nm) to protofibrils (4.0 nm) to fibrils (8.0 nm) in diameter was proposed (7). A system has been devised for *in situ* AFM observation of fibril formation using a fluid cell with mica as the supporting substrate. This *in situ* system permits observation of the time course of fibril formation. Thus, various transient aggregation species, such as oligomers, protofibrils, as well as mature fibrils, can be observed by AFM (19, 22, 23, 27, 28). In one reported case, the final fibril diameter and morphology observed on mica were different from those observed when fibrils were grown in solution (23). The current study also demonstrates that care must be used when comparing the results from *in situ* experiments in which the fibrils are grown on a surface and *ex situ* experiments in which the fibrils are grown in solution because the fibril formation process may be surface-dependent.

The present work focuses on the morphology of SMA aggregates deposited on surfaces as a function of time of incubation. The adsorption of protein on the surface was studied and correlated with fibril formation. Based on the data, a model for SMA fibril assembly is proposed.

MATERIALS AND METHODS

Protein Purification—The SMA expression system was a gift from Dr. Fred Stevens (Argonne National Laboratories). The recombinant variable domain SMA was purified following the reported protocol (1, 7, 8). Briefly, overexpressed protein was extracted from periplasm using sucrose and water. The extract was dialyzed in 10 mM acetate buffer (pH 5.6) and loaded on a SP-Sepharose Fast Flow column (Amersham Biosciences). The protein was eluted using 10 mM phosphate buffer (pH 8.0). The purity of the 2-ml fractions collected was assessed by SDS-PAGE. The purest fractions were pooled and concentrated by Centriprep R (10,000 molecular weight cutoff) and filtered through 0.22-μm filters before being stored in glass vials. Protein concentrations were measured via $A_{280\ nm}$ using the extinction coefficient of $E^{0.1\%} = 1.8$. The purity of the protein was assayed by SDS-PAGE.

In Vitro Fibril Formation on the Surface and in Solution—A filtered protein sample (0.22 μm) was treated with 0.001 M NaOH for 15 min to remove any preformed aggregates, then adjusted to a lower pH. Fibrils were grown from purified protein at a concentration of 50 μg/ml in 120 μl of solution with a piece of freshly cleaved mica (4 × 4 mm) in a plastic vial. The solution was incubated at 37 °C without agitation. Fibril growth experiments in mica-free solution involved incubating 50 μg/ml purified protein at 37 °C with shaking at 960 rpm. The standard buffer solution included 20 mM HCl (pH 2.0), 20 mM HEPES (pH 5.0), or 20 mM Tris-HCl (pH 7.4), with 200 mM NaCl. Fibril formation was monitored using light scattering and a fluorescence assay based on the enhanced fluorescence of the dye thioflavin T (ThT) on binding to amyloid fibrils (20, 21, 29). Both Rayleigh light scattering and fluorescence intensity were measured using a Fluoromax-2 (Jobin-Yvon/SPEX Inc.) spectrofluorometer. At each point time, a 220-μl sample was removed to measure Rayleigh light scattering at 330 nm with a 1-nm bandpass for both excitation and emission monochromators. ThT binding assays were conducted by adding a 10-μl sample to 990 μl of 20 μM ThT in 50 mM Tris-HCl (pH 7.4) and 100 mM NaCl. The fluorescence intensities were measured at 482 nm with excitation at 450 nm using a 5-nm bandpass on both the excitation and emission monochromators. In some experiments, fibrils were produced by incubating the same solution containing 4 μM ThT at 37 °C and agitation at 600 rpm with a shaking diameter of 1 mm. Fluorescence intensity was recorded *in situ* at 15-min intervals using a Fluoroskan Ascent CF (Thermo Labsystems, Finland) plate reader with emission at 482 nm and excitation at 444 nm. Teflon-coated stir bars or beads were used to increase the agitation.

Modification of Mica—Mica was alkylamine functionalized with 4-aminobutyl triethoxysilane to form a positively charged surface following the literature method (30) and modified with octadecyltrichlorosilane to form a hydrophobic surface following the reported method (31). Both were purchased from Gelest, Inc. (Tullytown, PA).

Adsorption of SMA on the Surface—Plastic vials (United Scientific Products) and quartz cells for UV measurements were treated with 1 mg/ml bovine serum albumin in 20 mM Tris buffer solution (pH 7.4) for 5 h before use. After such treatment, SMA did not absorb to the vial or cell as determined by measuring the concentration of protein in solution after a 24-h incubation at 37 °C. A mica sheet (4 × 4 mm) was put into the treated tube containing 120 μl of 0.5 mg/ml SMA in 20 mM Tris-HCl buffer solution (pH 7.4) containing 200 mM NaCl and incubated at 37 °C. At each sample time point (see below), the protein concentrations were measured by $A_{280\ nm}$. The adsorption of protein on the mica and stir beads was estimated by subtracting the protein concentration in solution from the total concentration.

AFM Measurements—Mica was removed at each time point from one of the incubation vials described above for AFM measurements, while a 5-μl aliquot from the same vial was transferred to a freshly cleaved mica surface at the same time. The mica-adsorbed samples were washed with water to remove unbound protein and dried with N_2 or air-dried overnight. AFM imaging was performed with an Autoprobe CP Multiple AFM (Park Scientific) in noncontact (tapping) mode. Measurements were carried out using silicon cantilevers with a spring constant of 50 newtons/m (Park Scientific) and a resonance frequency of 290–350 kHz. The images were acquired using the 100-μm Scanmaster and 5-μm scanner for high resolution imaging at a scan rate of 0.5 Hz for both scanners. All images were captured at 512 × 512 scans. Height sizes in the range of 2.5–50 nm were estimated by section analysis using the PSI program without calibration, and lateral sizes in the range of 10–100 nm were calibrated with various standard gold colloid particles using the same type of probe and similar set point for imaging. Some of the images were modified using SPIP software (Image Metrology, Denmark). At least four regions of the mica surface were examined to verify that similar structures existed throughout the sample.

RESULTS

In our previous study of SMA aggregation in solution, SMA formed typical fibrils over the range of pH 8.0–2.0; however, the yield of fibrils increased with decreasing pH. Fibrillation competed with the formation of amorphous deposits at all pH values, but the latter was negligible at low pH (*e.g.* pH 2). At pH 5.0 amorphous aggregates were the predominant aggregated material, and few fibrils were observed under these conditions (8).

To investigate the potential role of surfaces in amyloid fibril formation we incubated small pieces of mica in solutions of SMA, typically under conditions (low protein concentration, no agitation) where fibrils were not formed over a time period of a week or longer in bulk solution. The time course of aggregation was followed by imaging the mica surface after removal from the incubation solution using AFM. By chemically modifying the surface of the mica it was possible to change the nature of the surface, both in terms of net charge and also hydrophobicity.

When small (4 × 4 mm) sheets of mica were incubated (without agitation) in solutions of SMA at pH 5.0, 37 °C, amorphous aggregates were observed within a short time of incubation, and fibrils were observed starting around 10 h. These results were obtained with protein concentrations of 50 μg/ml, conditions under which no fibrils were formed in solution, thus indicating a strong accelerating effect of the surface. For much of the incubation period different types of aggregate were visible on the mica surface, indicative of multiple concurrent processes. Two major sources for fibrillar material were observed, discussed in detail below: 1) fibrils growing of amorphous aggregates, which was the predominant fibrillation process; and 2) fibrils assembling from oligomers. Neither of these processes is commonly thought of as a fibrillation mechanism, although there is precedent for the former (19, 22).

Fibrils Grow from Amorphous Aggregates—In the present study we noticed an interesting phenomenon on the mica surface, namely the formation of fibrils growing out of amorphous aggregates; we will call this fibril assembly mechanism 1. At early times (2–4 h), SMA samples prepared at pH 5.0 showed the presence of spherical amorphous deposits on the mica surface with heights in the range of 18–90 nm (Fig. 1*A*). By 12 h, as illustrated in Fig. 2, these amorphous spheroids had one to nine "fibrils" growing from them. Based on the height of the fibrillar material, about 5.0 nm, we will call these protofibrils (7). After 8 days, typically more than 10 protofibrils were radi-

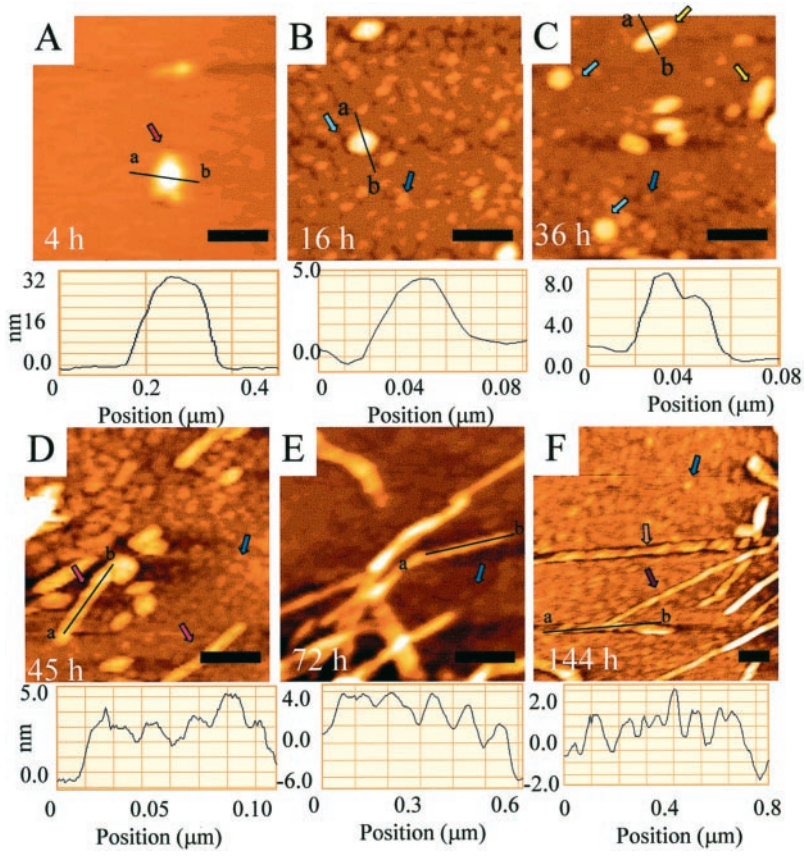

FIG. 1. **Time course of SMA aggregation on a mica surface at pH 5.0, 37 °C, showing fibril assembly mechanism 2.** AFM images were obtained using tapping mode, the lighter the color the higher the object. The protein concentration was 50 μg/ml. The time point of each image is indicated. Only amorphous aggregates were observed at 4 h with height in the range of 18–90 nm (*red arrow* in *A*). Single aggregate units (18 nm wide) (*green arrows*, *B*) self-assemble to form protofibrils composed of two (*yellow arrows*, *C*) or multiple aggregate units (*pink arrows*, *D*). Subsequently, some protofibrils rearrange and twist to form mature fibrils (*orange arrow*, *F*). Subunit aggregates with height around 2 nm (*blue arrows*) and a few 2.4-nm high protofilaments (*purple arrows*) were also observed. *Scale bars* are 200 nm. The *y* axis is 1 μm for *A–E* and 2.5 μm for *F*. The cross-section of the *line a–b* is shown below each *panel*.

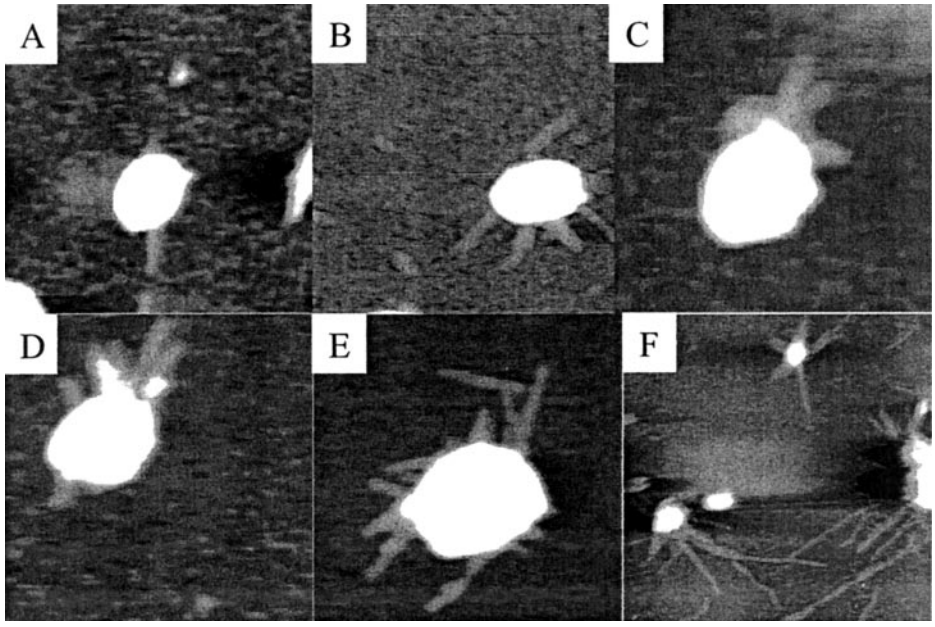

FIG. 2. **AFM images of SMA fibrils growing from amorphous aggregates on mica surfaces at pH 5.0, showing fibril assembly mechanism 1.** One (*A*), four (*B* and *C*), six (*D*), or nine (*E*) protofibrils radiated out from the central core by 12–16 h. The elongation of protofibrils leads to mature fibrils after 6 days (*F*). The *y* axis is 1 μm for *A–E* and 5 μm for *F*. The large difference in height (lighter color represents larger heights) between the amorphous aggregates and the (proto)fibrils leads to decreased resolution of the much smaller protofibrils. Conditions were pH 5.0, 50 μg/ml protein, 37 °C.

ating from the central amorphous core. The lengths of the protofibrils increased from around 100 nm at 12–16 h to several μm in 6 days (Fig. 2*F*). However, the height of the fibrils remained constant at 4.8 ± 0.8 nm at all times. The size of the amorphous aggregates increased over the first 20 h but then appeared to remain relatively constant until finally decreasing at longer times (≥6 days). The protofibrils radiating from the amorphous core were linear and smooth; no branched fibrils were observed. After 6 days only a few of these protofibrils were twisted to form fibrils with distinct periodicity, probably because of spatial hindrance and association with the mica surface. One end of these protofibrils was tightly associated with the original amorphous core, and no cleavage from the core occurred. This observation indicates strong attachment of the fibrils to the amorphous aggregates. At all times (after 8–10 h) the amorphous aggregates with radiating protofibrils were the predominant aggregated species observed. The initial appearance of amorphous aggregates, followed more slowly by fibrillation, is consistent with solution experiments with SMA, in which amorphous aggregation appeared before fibril formation at pH 5.0. Using light scattering we were unable to find evidence for amorphous aggregate formation in solution under these experimental conditions; however, small aggregates might not be detected under the conditions used, especially at

TABLE I
Dimensions of SMA oligomeric units and fibrils grown on mica at pH 5.0
The protein concentration was 50 μg/ml; temperature was 37 °C, no agitation.

Time	Height	Width	Length
h	*nm*	*nm*	*nm*
16	5.5 ± 0.5	18 ± 1	16–18
36	5.4 ± 0.8	17 ± 2	18–90 (1–5 units)[a]
45	4.8 ± 0.5	18 ± 2	35–140 (2–8 units)[a]
72	4.5 ± 0.5, 2.4 ± 0.2	22 ± 2, 14 ± 1.2	≤ 400 (about 20 units)[a]
144	4.3 ± 0.3, 2.4 ± 0.3	22 ± 1, 12 ± 0.5	500 nm–1 μm

[a] One unit corresponds to a single disk-like oligomer, as seen at 16 h, and corresponds to approximately 20 monomers.

the very low protein concentrations involved. Attempts to use size-exclusion chromatography high performance liquid chromatography to detect oligomers failed because of the SMA sticking to the column.

Assembly of SMA to Form Oligomeric Units—A second, slower mechanism of fibril formation was observed on mica at pH 5.0. By 16 h the AFM images revealed relatively uniform disk-shaped particles (Fig. 1*B*). These are oligomeric deposits of defined size (Table I), corresponding to 20–24 individual SMA molecules (assuming a molecular volume similar to that of the native state). We will call these oligomeric units aggregation building block units, for reasons that will become apparent. Subsequently, pairs of these oligomers fuse over the 16–36-h range, as discussed below (Fig. 1*C*).

The dimensions, including heights and lateral sizes of aggregates formed on the mica surfaces, were quantified by section analysis, and the results are shown in Table I. The lateral sizes of the samples were strongly influenced by the tip geometry. Hence, they were calibrated in terms of tip radius with the methods reported previously (32, 33) and further confirmed by standard gold particles and electron microscopy data. The size homogeneity of the disk-shaped particles was examined by measuring the height distributions (Fig. 3), which were well represented by Gaussian curves. The aggregation building block units were ~5.5 nm high (range 4.2–6.0 nm) and 15–18 nm wide. It is possible that these oligomeric units are initially spherical but adopt a flat (disk-like) structure on the charged surface because of the strong interaction between the protein and the surface.

In addition to the 5.5-nm high disk-shaped aggregates, small spheres of about 2-nm diameter are seen in the background starting at around 12 h (Fig. 1). It is possible that these are present at earlier times but not visible in the AFM image because of the much greater height of the amorphous aggregates. The size of these small species is in the range expected for native monomers of SMA (4.0 × 2.8 × 1.3 nm) or dimers. It is likely that these are not in the native conformation because of interactions with the surface. The number of these small spheres increased with increasing incubation time, suggesting increasing numbers of tightly adsorbed monomer/dimers with time and that they may be too tightly bound to participate in aggregation and fibrillation, *i.e.* the off-rate is very slow.

Elongation of Oligomeric Aggregation Units and Protofibril Formation—The 5.5-nm oligomeric aggregation units appear to serve as the building blocks for the formation of protofibrils, which grow from a single aggregation building block of SMA over a time of ≈45 h (Fig. 1, *C* and *D*). We use the term *protofibril* rather than *protofilament* because the size and morphology resemble the protofibrils observed in solution (7). A significant increase in the number of large (longer) aggregated species was observed from 36 to 45 h. The length of linear aggregates was typically between 18 and 400 nm. The larger ones were exactly integer multiples of the size of the oligomeric building block units, composed of 2–8 such units, and retained a basically constant height and width (Table I). These observations suggest that the aggregation building block unit is the basic unit of fibrillar assembly on the mica surface, and we will call this process fibril assembly mechanism 2. These individual units then assembled by linear association to produce the protofibrils in the presence of excess single units (Fig. 1*D*). Small numbers of single units fusing together are shown in Fig. 4. The growth of protofibrils was bidirectional and linear, and no branched aggregates were observed. Protofibrils were already growing from the amorphous core by 10 h (fibril assembly mechanism 1), a shorter time than that required for linear protofibril formation (fibril assembly mechanism 2). At 16 h the presence of various aggregated species, including the disk-like oligomeric building block units, amorphous aggregates, and protofibrils grown from the linear assembly of the aggregation building block units, were seen. A similar association of Aβ peptide oligomers, occurring at the early stages of aggregation, has also been reported recently (19, 22).

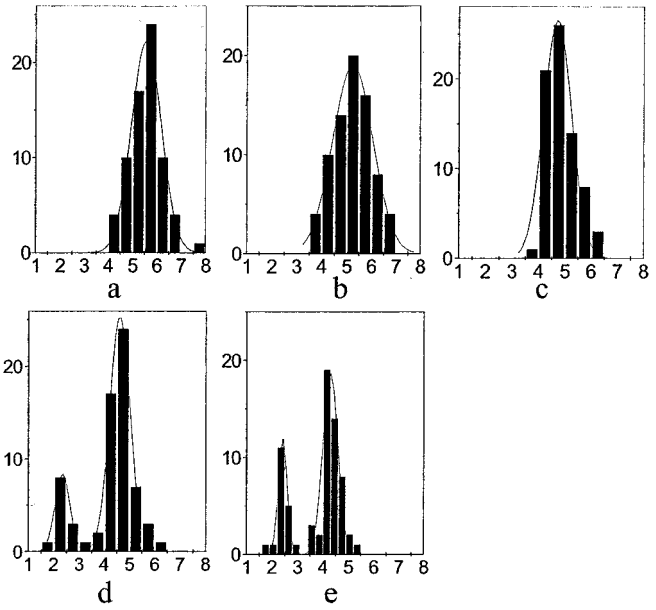

FIG. 3. **Height distribution of SMA fibrils and protofibrils grown on mica at pH 5.0 at 16 h (*a*), 36 h (*b*), 45 h (*c*), 72 h (*d*), and 144 h (*e*) (corresponding to the *panels* in Fig. 1).** The distribution has been fitted with Gaussian curves.

Elongation and Self-twisting of Protofibrils and Formation of Fibrils—Although retaining a constant height and width, the protofibrils formed by fibril assembly mechanism 2 continued to elongate over 3 days to form fibrils, which had a characteristic linear structure reaching lengths often exceeding 1 μm (Fig. 1, *E* and *F*). Heights were in the range of 4.0–5.4 nm, and the most prominent heights were 4.5 nm at 72 h and 4.3 nm at 144 h, which were slightly lower than the size of the protofibrils (4.8 nm). The widths also remained in the range of 20–23 nm, which was slightly larger than for the protofibrils (18 ± 2 nm). We noticed that the heights of all of the aggregates were sim-

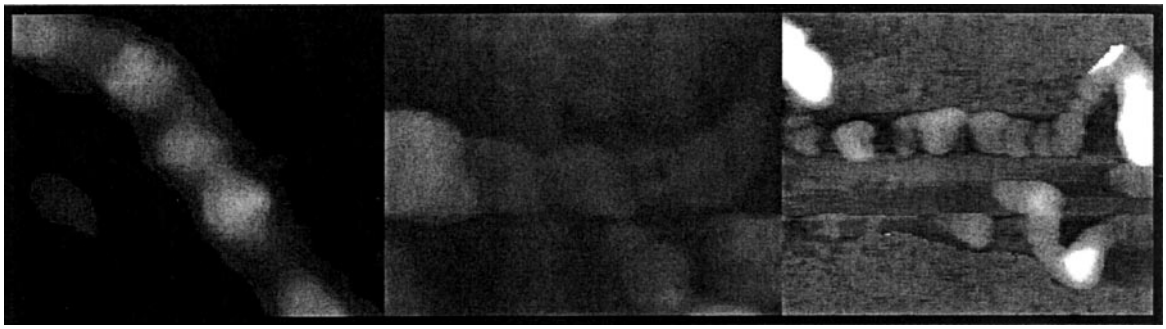

FIG. 4. **Representative AFM images showing fibril assembly mechanism 2, in which the aggregation building block oligomers assemble linearly into protofibrils.** Conditions were pH 5.0, 50 μg/ml protein, 37 °C.

ilar but decreased from 5.5 nm to 4.3 nm step by step in the pathway of fibril formation. Section analysis across the axis of protofibrils formed at 36 h (Fig. 1*C*, *lower panel*) indicated a hollow in the center of the disk-shaped particles. This could reflect the initial event leading to the periodic twisting observed in longer fibrillar species at later times. Analyzing longitudinal sections (along the fibril axis) of fibrils showed the existence of an axial periodicity of $\approx$ 100 nm (Fig. 1, *D* and *E*). An additional periodicity of 38 $\pm$ 5 nm in fibrils occurred at 144 h on the mica surface (Fig. 1*F*). The fibrils seemed to twist more and more tightly while both the height and periodicities decreased. The adsorption of protein on the surface and the resultant "spreading" may contribute to the slight expansion of lateral sizes. The height of the mature fibrils grown on mica (3 and 6 days) was similar to that of protofibrils grown in solution (7). The distinct rope-like morphology was only observed in the final fibrillar structures at long time points (144 h) and for relatively few fibrils. This probably reflects a slow rearrangement in the fibril morphology. It is likely that the tight binding of the protofibrils to the surface will impede any tendency to twist around each other, as might readily occur in solution. Thus, fibril formation on the mica surface by this second assembly mechanism involves the linear association of oligomeric units to form protofibrils, which may undergo subsequent "intrafibril" morphological rearrangements to give twisted fibrils 4.3 nm high. This is a very different mechanism than that observed for fibril formation in solution, in which elongated protofilaments interact with each other to form protofibrils and fibrils with twisted structures (7).

A few 2.4-nm high fibrils were observed at 72 h on the mica surface with a width of 12–14 nm (Table I), corresponding to the protofilaments seen in solution incubations. These protofilaments may lead to the twisted 4.3-nm protofibrils, as shown in Fig. 1*F*. The protofilaments could arise from monomer/dimer species directly because the height of the protofibril is the same as the small spheres shown in Fig. 1, *B–D*. Alternately, these protofilaments could arise from splitting of the 4.3-nm fibrils because the height and width of the newly formed filamentous material were exactly half those of the linear assembled protofibrils grown from the aggregation building block units. The central "caved in" structure shown in the *lower panel* of Fig. 1*C* may support this assumption.

The Morphology of Fibrils Formed on the Mica Surface Was Affected by pH—To evaluate the effect of pH on the morphology of fibril formation, mica was also incubated in 50 μg/ml SMA solutions at pH 2.0 and 7.4. AFM measurements were carried out after removal of the mica from the incubation solution as a function of time. Incubation of mica at pH 2.0 for 7 h yielded predominantly particles having a height of 2.4 $\pm$ 0.3 nm and a width of 6–8 nm, which is consistent with monomer/dimers (Fig. 5*A*). The density of adsorbed protein on mica was much higher at pH 2.0 than at pH 5.0. After incubating the sample

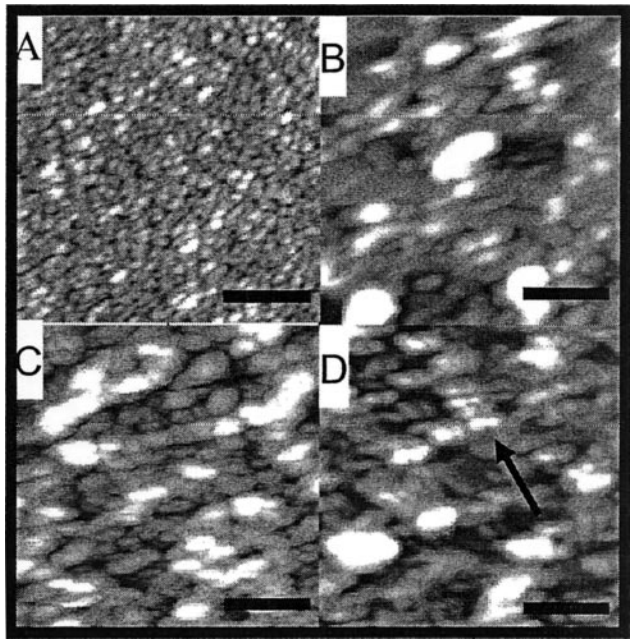

FIG. 5. **AFM images of the time course of SMA aggregating on mica surfaces at pH 2.0.** *A*, 7 h; *B*, 16 h; *C*, 65 h; *D*, 122 h. The *arrow* in *D* shows a series of aligned linear aggregates. Conditions were 50 μg/ml protein, 37 °C. The *y* axis is 2 μm, and the *scale bars* are 200 nm.

for 16 h, both small and large aggregates were observed in the pH 2.0 preparation (Fig. 5*B*). However, by 65 h the aggregates had a uniform size of 4.8 $\pm$ 0.3 nm high and 16–19 nm wide (Fig. 5*C*). A significant population of the 4.8-nm height aggregation units at 65 h was aligned to some extent to form nascent protofibrils (Fig. 5*D*). Sometimes two or three such ordered assemblies were aligned side by side (Fig. 5*D*, *arrow*). Nevertheless, the aggregates of SMA at pH 2.0 were mostly unordered, and no typical linear fibrils were seen.

At pH 7.4 (100 mM NaCl in 20 mM Tri-HCl buffer), oligomeric deposits of SMA of $\approx$ 5-nm height and 16 $\pm$ 1-nm width appeared at 6 days, and subsequently larger amorphous aggregates were found, rather than fibrils (data not shown). Amorphous aggregates, as well as fibrils, are typically found for SMA at pH $\geq$ 7 in solution. The experiments on mica showed no distinct fibrillar structures on the surface at pH 7.4.

No Fibrils Were Formed in Solution under Similar Conditions—After the removal of the incubated mica sheets, aliquots of incubation solution at pH 2.0 and pH 5.0 were transferred to freshly cleaved mica for AFM measurements as well as ThT binding assays. ThT binding is a general indicator of fibril formation (9). The lack of increase in ThT fluorescence on addition of the protein solution to ThT suggested that no fibrils were present in the solution and also that no fibrils broke off

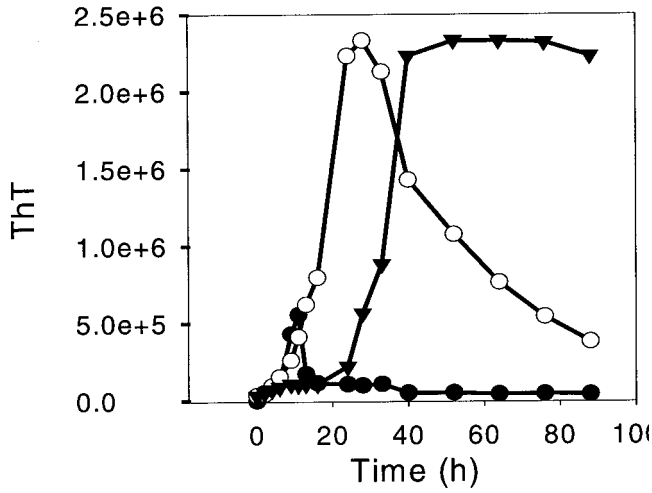

FIG. 6. **Concentration-dependent kinetics of SMA fibrillation in solution.** SMA at 0.05 (*solid circles*), 0.2 (*open circles*), and 0.5 mg/ml (*solid triangles*) in 20 mM Tris buffer containing 200 mM NaCl, pH 7.4, was incubated at 37 °C in glass vials with shaking at 960 rpm. A 10-μl aliquot of SMA was removed and added to 990 μl of ThT solution, and the fluorescence was measured as described under "Materials and Methods."

the mica surface. In confirmation, no fibrillar material was observed by AFM imaging.

SMA was incubated in solution under the same conditions (no agitation) as for the mica surface experiments. In contrast to the results in the presence of mica surfaces, both the ThT assay and AFM imaging showed the absence of fibrils with 50 μg/ml SMA incubated at pH 2.0 and pH 5.0.

When the incubation conditions were modified to include shaking at 960 rpm, the kinetics of aggregation, monitored by ThT fluorescence, were as shown in Fig. 6 (lowest curve for 50 μg/ml). The ThT fluorescence profile initially showed a characteristic nucleation-dependent polymerization pattern, having a lag phase followed by a rapid growth phase, but subsequently decreased immediately after reaching the maximum. Aliquots of incubation solution were taken as a function of time for AFM measurements. The AFM data showed that some small aggregates appeared after incubation for 24 h, but only at 0.2 mg/ml SMA. Further association of these particles formed larger aggregation units at 28 h, the time of maximal ThT signal in the kinetics curve for 0.2 mg/ml SMA. At longer times disassembly of these aggregation units occurred. No aggregation building block units and no protofibrils were detected in AFM imaging in these samples. This was consistent with the decreasing ThT signal in the kinetics curve. The nonfibrillar aggregates at low concentrations of SMA were also confirmed by electron microscopy data. When the concentration of SMA was increased to 0.5 mg/ml, a typical sigmoid shape with a lag phase followed by a significant increase and then constant plateau was observed by ThT, instead of the bell-shaped kinetics shown in Fig. 6 at the low SMA concentration. The critical elongation concentration for SMA was determined to be 0.3 mg/ml, and typical fibrils were seen by AFM imaging when the initial concentration was $\geq$0.3 mg/ml.

Adsorption of Protein on Various Surfaces and Its Correlation with Fibril Formation—The adsorption of SMA to various surfaces, including untreated negatively charged mica, positively charged modified mica, and mica modified to have a hydrophobic surface, as well as hydrophobic Teflon, were examined at pH 2.0, 5.0, and 7.4, with the results shown in Fig. 7. Essentially no protein adsorption occurred on the hydrophobic surfaces, which probably accounts for the lack of fibrillation on hydrophobic surfaces. Interestingly, similar amounts of protein adsorption occurred on both negatively charged and positively charged surfaces at pH 2.0 and 7.4, probably reflecting both hydrophobic and electrostatic effects in binding. At pH 2.0 and 7.4 adsorption was saturated at 50 μg/ml, and no more SMA was adsorbed after the first molecular layer of mica (data not shown). Thus, the same amount of protein was adsorbed at both 0.05 and 0.3 mg/ml. However, at pH 5.0, there was still further adsorption on the surface when the concentration of protein was increased from 50 μg/ml to 0.3 mg/ml. Because the surface was completely covered by protein molecules after the first layer of adsorption, SMA molecules were being adsorbed onto the surface-immobilized protein rather than the mica surface. This suggested that at this pH SMA adsorbed on the mica surface in a conformation that favored association with other proteins, and more and more protein molecules or aggregates bound to the initially immobilized protein from the solution. Therefore, the local concentration of SMA would be increased greatly, and the fibrils were formed from the protein pool on the surface.

Fibrils Formed on the Surface Are Very Stable—We noticed that the fibrils formed on mica surfaces were not broken off during the incubation process, and no fibrils were observed in the incubation solution. After the fibrils were formed on mica (6 days), we transferred the mica sheet to the buffer solution and continued to incubate it at 37 °C for 1 week. The mica sheet was then removed from the solution and rinsed with water to move the unbound protein for AFM measurements. The solution was examined for all types of protein structures, including native protein, protofibrils, or fibrils, by absorbance at 280 nm, ThT binding assays, and AFM imaging. No protein was detected in solution, which means there was no release of protein from the surface. AFM images showed that the fibrils remained unchanged on the mica surface. This confirms the strong interaction between SMA and the mica surface.

DISCUSSION

The results reported here indicate that surfaces can catalyze the formation of amyloid fibrils and that the mechanism of surface-induced fibrillation may be significantly different from that occurring in bulk solution. In solution, a hierarchical assembly mechanism is observed for SMA fibrillation (7). This involves the initial formation of protofilaments of 2.4-nm diameter, two of which intertwine to form protofibrils of 4.0-nm diameter at intermediate times, followed by the twisting together of two protofibrils to form type I mature fibrils of 8.0 nm. The latter two forms show typical twisted rope-like morphology. Occasionally, under some conditions, type II fibrils of 6.0-nm diameter and composed of three protofilaments were observed.

Both Small Oligomeric Units and Amorphous Aggregates Are Intermediates in the Surface Assembly of SMA Fibrils—The current work demonstrates that fibrils can assemble on mica at quite low protein concentrations and much lower than required for fibril formation in solution under comparable conditions. The kinetics of SMA fibril formation, monitored by AFM, showed that amorphous aggregates (20–100-nm diameter) were formed within 4 h, and uniform disk-shaped oligomeric units appeared by 12–16 h. Both served as sources of fibrillar material, which exhibited different types of morphology. Based on their heights of around 5 nm, we classify the fibrillar material as protofibrils. These were formed either by linear assembly of the disk-shaped oligomeric units (fibril assembly mechanism 2) or grew out from the amorphous aggregates (fibril assembly mechanism 1). Fibril formation from the amorphous aggregates was initiated much more rapidly than the linear assembly of the disk-shaped oligomers.

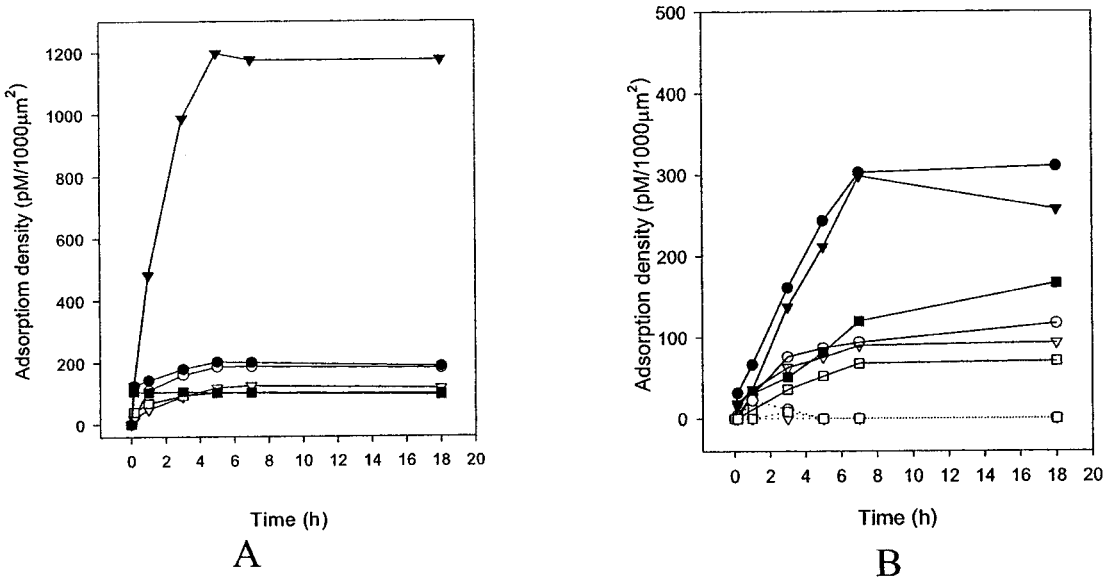

FIG. 7. **SMA adsorption to mica and modified mica surfaces.** SMA, 50 μg/ml (*open symbols*) or 0.3 mg/ml (*solid symbols*) was adsorbed on 4 × 4-mm unmodified mica (*A*), positively charged, modified mica (*B*, *solid lines*), or hydrophobic surface-modified mica (*B*, *dotted lines*) at pH 2.0 (*circles*), 5.0 (*triangles*), or 7.4 (*squares*) in the presence of 200 mM NaCl, 25 °C.

The first aggregated species observed were the spherical amorphous aggregates; these could arise either by initial formation in bulk solution followed by adsorption to the mica surface, or by direct growth on the mica surface. In either case we assume that they result from association of the I_N intermediate (8). Unfortunately, we were unable to determine unambiguously whether the initial aggregates arose from solution or on the surface. The apparent lack of smaller amorphous aggregates on the mica surface and the fact that amorphous aggregates of SMA form quite rapidly in solution at pH 5 (8) may indicate that they arise from bulk solution; however, we suspect that formation of the amorphous aggregates is catalyzed by the surface. At pH 2, where little amorphous material is observed in solution, no early surface-adsorbed amorphous aggregates were observed. The kinetics of protein adsorption to the surface indicate that at pH 5 the mica surface became "saturated," corresponding to about 60% of the total protein (for 50 μg/ml) being on the surface (Fig. 7). This suggests either an equilibrium between adsorbed and dissolved SMA or most likely a limited number of protein sites on the surface.

The observation of the formation of fibrils growing out from the amorphous aggregates indicates that amorphous aggregates may act as nuclei for fibril formation. This confirms an intermediate role of the amorphous aggregates and suggests that the amorphous aggregate also provides specific fibril initiation sites.

The intermediate role of the amorphous aggregates in fibril formation is a new hypothesis that may lead to a clearer understanding of the role of amorphous aggregates in amyloidogenesis. This is particularly significant, in that many fibrillation systems may also involve (transient) amorphous aggregates. Millhauser and co-workers (34) have reported that amyloid formation from a prion peptide required the presence of the amorphous aggregate. The formation of disk-shaped spherulites of LC domains was observed *in vitro* by Congo Red birefringence. The Maltese cross extinction of the Congo Red-stained samples suggested a radial arrangement of fibrils in the spherulites (11). The spherulites have also been observed in tissue sections from patients with LC amyloid disease (35). Radial growth of Aβ40 peptide fibrils from a central core has been observed by AFM (19).

Fibril Formation Is Accelerated by Surfaces—The critical concentration for SMA fibrillation decreased from 0.3 mg/ml in solution to lower than 50 μg/ml on the mica surface. Considering that the surface fibrillation conditions did not involve such critical factors as stirring or shaking, the surface-induced fibrillation is orders of magnitude faster than that in solution. There are several possible explanations. The adsorption of protein on the surface may increase the concentration of protein in local surface regions, and increasing protein concentration normally increases the rate of fibrillation. It is possible that two-dimensional lateral diffusion on the surface affects the fibril assembly process; it is known that polymers can undergo rapid lateral diffusion on surfaces. The presence of stable amorphous aggregates, which may serve as nucleation sites for fibril growth, and the fact that the kinetics of this process are relatively fast, could contribute to the fast growth of fibrils. It is most likely that adsorption of the protein on the surface induces conformational change, presumably to a partially folded intermediate that is critical for protein association. If the intermolecular forces between protein molecules in the amorphous aggregates are weaker than those in fibrils, as is likely to be the case, then the high local concentration of protein in the amorphous deposit could well act as a reservoir for fibril formation. Finally, the apparent association of the "aggregation building block units," specific oligomers, to form protofibrils is a process that has not been observed in the corresponding solution incubations and may thus represent an alternative mechanism for fibrillation with faster kinetics.

Model for SMA Assembly on Surfaces—The current AFM observations suggest a model to account for SMA surface fibrillar assembly at pH 5.0, shown in Fig. 8. Previous studies suggest that the underlying kinetic reaction scheme for the formation of SMA fibrils in solution involves the following major steps:

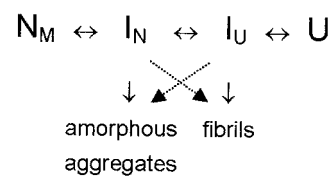

SCHEME 1

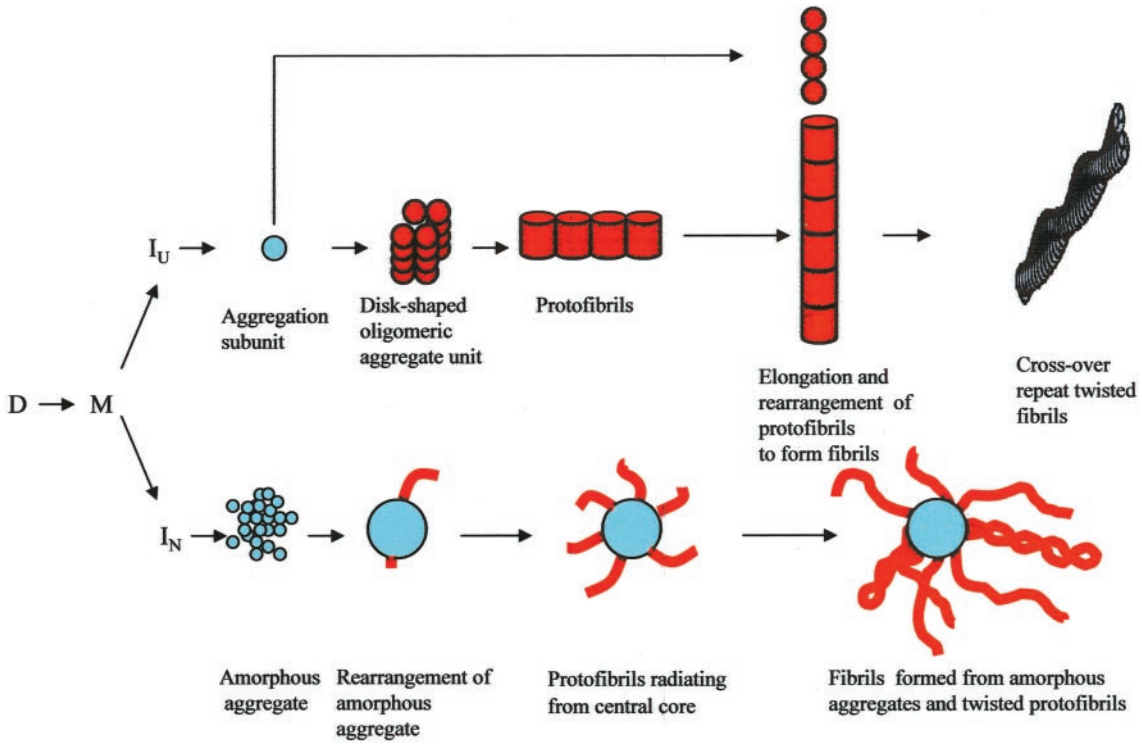

FIG. 8. **Schematic model outlining a possible mechanism for SMA fibril formation on surfaces.** The aggregation subunit is probably I_U, or an oligomer of I_U (see "Results"). The *upper pathway* shows assembly mechanism 2, and the *lower pathway* shows assembly mechanism 1.

where N_M corresponds to the native monomer, I_N is a relatively native-like intermediate, which leads predominantly to amorphous aggregates, and I_U is a relatively unfolded intermediate, which readily forms amyloid fibrils (8). Critical aspects are the necessity for a partially folded intermediate for aggregation and the presumed presence of a transient nucleus formed from the association of the I_U intermediates to form fibrils (initially protofilaments of 2.5-nm diameter), as well as the concurrent formation of amorphous aggregates under many conditions. Any dimeric SMA must initially dissociate into the monomer; at the low SMA concentrations (50 μg/ml) used in most of the experiments described here, there will be predominantly monomer present because the K_d values range from $\approx$10 μM at pH 7 to $\approx$60 μM at pH 2.

SMA fibrillation on mica surfaces reveals two apparently quite different pathways. In one, disk-shaped oligomers of $\approx$20 SMA molecules assemble on the surface, presumably in a partially folded conformation (I_U) in Fig. 8. At this stage we cannot determine whether these oligomers form in solution or on the surface of the mica, but the latter seems more likely. These oligomers serve as building block units for the assembly of protofibrils, by self-association through dimeric, trimeric units etc. The elongation of the initially formed short protofibrils involves the addition of further oligomeric units. At long time periods there appear to be internal rearrangements in which the protofibrils form cross-over repeat structures. A similar mechanism for fibril formation by the linear association of oligomeric building blocks on a surface has been reported for Aβ (19).

The alternate pathway involves fibrils growing out from amorphous aggregates, which are much larger than the oligomeric building blocks. The amorphous aggregates most likely arise from relatively rapid nonspecific association of the I_N intermediate in solution, probably via exposed hydrophobic patches. The subsequent rearrangement of the random structures in the amorphous aggregates leads to the formation of ordered fibrillar species. The mechanism suggested here explains why the amorphous aggregation appears earlier than fibril formation.

Fibril Formation Is Surface-dependent—The association of the protein with the surface clearly plays an important role in the formation of fibrils. Fibrils were formed on the normal negatively charged surface of mica, but no fibrils were observed when the protein was incubated with positively charged or nonpolar modified mica. This indicates that interaction between the protein and surface involves significant electrostatic interactions. Interestingly, the maximum interaction with the negatively charged mica occurred at pH 5.0, very close to the pI. Significantly less binding occurred at pH 2.0 and 7.4 to the positively charged surface. The lack of protein binding to the hydrophobic surface indicates that hydrophobic interactions play a relatively minor role. At high concentrations of NaCl, long distance van der Waals forces may play a role in the adsorption of protein on mica because of the screening of the charges by salt (36). The results demonstrate that monomers/dimers, small oligomers (aggregation building block units), sizable amorphous aggregates, and fibrillar species all bind strongly to the negatively charged mica surface, especially at pH 5. The interaction forces between monomer/dimer, and even the small oligomeric aggregation building blocks, must be sufficiently weak to allow lateral mobility leading to growth of aggregates and protofibrils on the surface. The affinity of SMA toward the slightly negatively charged surface of mica may be driven by amino acid residues located in the hydrophilic regions of the surface. We propose that there are surface-induced conformational changes on binding (to I_N and I_U) which favor the subsequent association of the protein, probably via hydrophobic interactions. There is precedent for such surface-induced conformational change, *e.g.* of human serum albumin to talc (38), and a drop-like, pseudo-micellar species of Aβ peptide on mica has been suggested (22, 37).

The majority of fibrillar species of SMA seen on the mica surface were smooth protofibrils, although some partially twisted and twisted protofibrils were seen; but larger diameter

mature fibrils, which are observed in solution incubations, were absent on the surface. The transition of the partially twisted fibrils to the twisted fibrils was a slow process in the surface fibrillation. Fibrillation/aggregation on a mica surface is probably much closer to the *in vivo* situation. In LC (AL) amyloidosis the most common sites of amyloid deposit are in the kidneys and the heart. It has been established that LC variable domains with sequences that lead to less stable native states are particularly prone to form amyloid deposits. It is very likely that it is a combination of the membrane surfaces in the heart, kidney, and blood vessels and the agitation in the last because of the high rate of blood velocity, and the destabilizing lower pH and higher salt and urea concentrations in the kidneys that lead to the *in vivo* deposits. The association of artificial (phospholipid) and β-lymphocyte membrane with an Igλ LC has been reported (15). Although the charge properties of the mica surface are close to those of the cell membrane, and mica is easily modified, it clearly has limitations as a model for biological membranes. Nevertheless, the key features, namely the aqueous-solid interface and the heterogeneous electronic properties of the solid surface, are common both to mica and lipid membranes. The investigation of SMA fibril formation on phospholipid bilayers is currently in progress. Additional complications with respect to *in vivo* fibrillation result from the fact that our results show that the kinetics of fibril formation are surface-dependent and surface-accelerated, and thus changes in the structure or components of cell surfaces, such as lipid oxidation, may significantly affect the fibril formation pathway and kinetics.

AFM opens up the possibility of obtaining information about the mechanism of fibrillation at the level of single building block units and contributing to the model accounting for the process of fibril formation. This is a great advantage over bulk measurements for recording fibril growth, such as ThT assays and light scattering, which average the properties of all fibrillar forms at once.

REFERENCES

1. Myatt, E. A., Westholm, F. A., Weiss, D. T., Solomon, A., Schiffer, M., and Steven, F. J. (1994) *Proc. Natl. Acad. Sci. U. S. A.* **91,** 3034–3038
2. Sasaki, A., Iijima, M., Yokoo, H., Shoji, M., and Nakazato, Y. (1997) *Brain Res.* **755,** 193–201
3. Solomon, A., Weiss, D. T., Murohy, C. L., Hrncic, R., Wall, J. S., and Schell, M. (1998) *Proc. Natl. Acad. Sci. U. S. A.* **95,** 9547–9551
4. Steven, F. J., and Argon, Y. (1999) *Immunol. Today* **20,** 451–457
5. Wall, J., Schell, M., Murphy, C., Hrncic, R., Steven, F. J., and Solomon, A. (1999) *Biochemistry* **38,** 14101–14108
6. Solomon, A., Weiss, D. T., and Kattine, A. A. (1991) *N. Engl. J. Med.* **324,** 1845–1851
7. Ionescu-Zanetti, C., Khurana, R., Gillespie, J. R., Petrick, J. S., Trabachino, L. C., Minert, L. J., Carter, S. A., and Fink, A. L. (1999) *Proc. Natl. Acad. Sci. U. S. A.* **96,** 13175–13179
8. Khurana, R., Gillespie, J. R., Talapatra, A., Menert, L. J., Ionescu-Zanetti, C., Millett, I., and Fink, A. L. (2001) *Biochemistry* **40,** 3525–3535
9. Kim, Y. S., Cape, S. P., Chi, E., Raffen, R., Wilkins-Stevens, P., Stevens, F. J., Manning, M. C., Randolph, T. W., Solomon, A., and Carpenter, J. F. (2001) *J. Biol. Chem.* **276,** 1626–1633
10. Wilkins-Stevens, P., Raffen, R., Hanson, D. K., Deng, Y. L., Berrios-Hammond, M., Westholm, F. A., Murphy, C., Eulitz, M., Wetzel, R., Solomon, A., Schiffer, M., and Stevens, F. J. (1995) *Protein Sci.* **4,** 421–432
11. Raffen, R., Dieckman, L. J., Szpunar, M., Wunschl, C., Pokkuluri, P. R., Dave, P., Wilkins-Stevens, P., Cai, X., Schiffer, M., and Stevens, F. J. (1999) *Protein Sci.* **8,** 509–517
12. Goldberg, M. S., and Lansbury, P. T., Jr. (2000) *Nat. Cell Biol.* **2,** E115–E119
13. Buxbaum, J. (1992) *Hematol. Oncol. Clin. North. Am.* **6,** 323–346
14. Buxbaum, J., and Gallo, G. (1999) *Hematol. Oncol. Clin. North Am.* **13,** 1235–1248
15. Lambert, M. P., Barlow, A. K., Chromy, B. A., Edwards, C., Freed, R., Liosatos, M., Morgan, T. E., Rozovsky, I., Trommer, B., Viola, K. L., Wals, P., Zhang, C., Finch, C. E., Krafft, G. A., and Klein, W. L. (1998) *Proc. Natl. Acad. Sci. U. S. A.* **95,** 6448–6453
16. Gallo, G., Goni, F., Boctor, F., Vidal, R., Kumar, A., Stevens, F. J., Frangione, B., and Ghiso, J. (1996) *Am. J. Pathol.* **148,** 1397–1406
17. Wall, J. S., Ayoub, F. M., and O'Shea, P. S. (1996) *Frontiers Biosci.* **1,** 46–58
18. Koo, E. H., Lansbury, P. T., Jr., and Kelly, J. W. (1999) *Proc. Natl. Acad. Sci. U. S. A.* **96,** 9989–9990
19. Blacky, H. K. L., Sanders, G. H. W., Davies, M. C., Roberts, C. J., Tendler, S. J. B., and Wilkinson, M. J. (2000) *J. Mol. Biol.* **298,** 833–840
20. Nielsen, L., Khurana, R., Coats, A., Frokjaer, S., Brange, J., Vyas, S., Uversky, V. N., and Fink, A. L. (2001) *Biochemistry,* **40,** 6036–6046
21. Naiki, H., and Gejyo, F. (1999) *Methods Enzymol.* **309,** 305–318
22. Kowalewski, T., and Moltzman, D. M. (1999) *Proc. Natl. Acad. Sci. U. S. A.* **96,** 3688–3693
23. Goldsbury, C., Kistler, J., Aebi, U., Arvinte, T., and Cooper, G. J. S. (1999) *J. Mol. Biol.* **285,** 33–39
24. Jo, E., McLaurin, J., Yip, C. M., St. George-Hyslop, P., and Fraser, P. E. (2000) *J. Biol. Chem.* **275,** 34328–34334
25. Yip, C. M., and McLaurin, J. (2001) *Biophys. J.* **80,** 1359–1371
26. Volles, M. J., Lee, J.-S., Rochet, J.-C., Shilerman, M. D., Ding, T. T., and Lansbury, P T., Jr. (2001) *Biochemistry* **40,** 7812–7819
27. Ding, T. T., and Harper, J. D. (1999) *Methods Enzymol.* **309,** 510–525
28. Stolz, M., Stoffler, D., Aebi, U., and Goldsbury, M. S. (2000) *J. Struct. Biol.* **131,** 171–180
29. LeVine, H., III (1993) *Protein Sci.* **2,** 404–410
30. Yang, Z., and Yu, H. (1999) *Langmuir* **15,** 1731–1737
31. Tang, Z., Jing, W., and Wang, E. (2000) *Langmuir* **16,** 1696–1702
32. Koutsos, V., van der Vegte, E. W., Grim, P. C. M., and Hadziioannou, G. (1997) *Macromolecules* **31,** 116–123
33. Koutsos, V., van der Vegte, E. W., Pelletier, E., Stamouli, A., and Hadziioannou, G. (1997) *Macromolecules* **30,** 4719–4726
34. Lundberg, K. M., Stenland, C. J., Cohen, F. E., Prusiner, S. B., and Millhauser, G. L. (1997) *Chem. Biol.* **4,** 345–355
35. Stokes, M. B., Jagirdar, J., Burchstin, O., Kornacki, S., Kumar, A., and Gallo, G. (1997) *Modern Pathol.* **10,** 1059–1065
36. Mueller, D. J. (1997) *J. Struct. Biol.* **119,** 172–188
37. Jackson Huang, T. H., Yang, D.-S., Plaskos, N. P., Go, S., Yip, C. M., Fraser, P. E., and Chakrabartty, A. (2000) *J. Mol. Biol.* **297,** 73–87
38. Van Oss, C. J., Docoslis, A., and Giese, R. F., Jr. (2001) *Colloids Surf.* **22,** 285–300